Journal of Environmental Chemical Engineering 9 (2021) 105804

Contents lists available at ScienceDirect

Journal of Environmental Chemical Engineering

journal homepage: www.elsevier.com/locate/jece

Phenol monitoring in water samples using an inexpensive electrochemical sensor based on pencil electrodes modified with DTAB surfactant

Gulsah Congur [a,b,*], U.Ülküye Dudu GÜL [a,b]

[a] Bilecik Seyh Edebali University, Vocational School of Health Services, 11230 Bilecik, Turkey
[b] Bilecik Seyh Edebali University, Biotechnology Application and Research Center, 11230 Bilecik, Turkey

ARTICLE INFO

Editor: Dr. G. Palmisano

Keywords:
Phenol
Electrochemical sensor
Pencil graphite electrode
Water analysis
Cationic surfactans
Dodecyltrimethylammonium bromide

ABSTRACT

Phenol (PNL) and phenolic compounds are major contaminants for water sources as they are used for the production of many industrial products. Herein, it is aimed to fabricate a novel voltammetric sensor platform for selective, sensitive, and practical detection of PNL. For this purpose, pencil graphite electrodes (PGEs) were modified with dodecyltrimethylammonium bromide (DTAB) surfactant as the first time in the literature. The optimizations of the experimental conditions for modification of DTAB at the surface of PGEs were done, then the oxidation signal of PNL was measured at +0.660 V using DTAB-PGEs. Enhanced PNL signal was obtained by using DTAB-PGEs and sensitive detection of PNL was achieved. PNL detection was successfully performed in not only buffer solution but also in tap water and industrial wastewater by reaching the detection limits as 0.16 μg/mL, 0.12 μg/mL, and 0.24 μg/mL, respectively. Moreover, DTAB-PGEs eliminated the interference effects of inorganic and organic compounds for the detection of PNL. This is the first study in the literature in terms of the development of DTAB-PGEs and non-enzymatic voltammetric detection of PNL by using DTAB-PGEs.

1. Introduction

Surfactants are organic compounds that have unique structures consisting a head group and a tail group. They are able to reduce the interfacial tension and they have the ability to form self-assembled structures [1]. They are used in many different areas including nanotechnology [2–6] and the use of surfactants for development of (bio) sensor systems by themself or in combination with different nanomaterials has been studied. Moreover, the development of electrochemical (bio)sensors by using cationic surfactants [7–15] and the number of reports about cationic surfactants based electrochemical (bio) sensors has been increasing day-by-day. The previous studies in this field were presented in Table 1 [8–21]. As represented in Table 1, cetyltrimethylammonium bromide (Synonym: hexadecyltrimethylammonium bromide; CTAB) [7,8,15–18] and dodecyltrimethylammonium bromide (DTAB) [9–14] are commonly used cationic surfactants into the electrochemical (bio)sensor area. Most of the modified surfaces are carbon-based electrodes, especially carbon paste electrodes (CPEs). However, the preparation of CPEs requires labor-intensive experimental steps such as preparation of homogenous carbon paste and filling of this paste into a glass tube, polishing and sonication. The preparation of glassy carbon electrodes (GCE) also requires polishing, and sonication pretreatment steps. These procedural necessities make CPEs and GCEs unfavorable to fabricate hand-held practical systems. Screen printed electrodes (SPEs) and pencil graphite electrodes (PGEs) are disposable carbon electrodes and can be prepared without the requirement of complex procedures and allowed to design model systems for lab-on-a-chip technologies. However, PGEs are more affordable than SPEs which makes them preferable. Moreover, they have a unique immobilization/adsorption surface for (bio)molecules due to their robust graphite structure which forms a high surface area [19]. CTAB in combination with gold nanoparticles (AuNPs) [17] or multi-walled carbon nanotubes (MWCNT) [18] was used for modification of PGEs. The modification of AuNPs/CTAB was done by the passive adsorption process [17] while MWCNT/CTAB was modified electropolymerization technique [18]. AuNPs/CTAB/PGE and MWCNT/CTAB/PGE have been used for the detection of cefixime or irinotecan (CPT-11) drugs, respectively. However, there is no report in the literature for modification of DTAB at the surface of PGEs.

Within the scope of the present study, a voltammetric sensor was developed by using disposable PGEs for the detection of PNL. To the best of our knowledge, there is no report in the literature for the development

* Corresponding author at: Bilecik Seyh Edebali University, Vocational School of Health Services, 11230 Bilecik, Turkey.
E-mail addresses: gulsah.congur@bilecik.edu.tr, gulsah.congur@gmail.com, gulsah.congur@hotmail.com (G. Congur).

https://doi.org/10.1016/j.jece.2021.105804
Received 9 April 2021; Received in revised form 19 May 2021; Accepted 2 June 2021
Available online 9 June 2021

Table 1
Surfactant modified electrochemical (bio)sensors. **Abbreviations:** BDD: Boron doped diamond, **PGCPE:** Pencil graphite carbon paste electrode, **CC:** Carbon ceramic, **CS:** Chitosan, **TTAB:** Tetradecyltrimethylammonium bromide, **SDS:** Sodiumdodecyl sulfate, **TFACl:** N-(1,1,2,2-tetrahydroperfluorooctyl)-N,N-dimethylammonium chloride, **SLS:** sodium lauryl sulphate, **MWCNT:** Multi-walled carbon nanotube, **PAn–SiO_2:** polyaniline–silica, **CNT:** Carbon nanotube, **RGO:** reduced graphene oxide, **NFC:** Nanofibrillated kenaf cellulose, **BPA:** bisphenol A, **HQ:** hydroquinone, **Mb:** Myoglobin, **NRF:** Norfloxacin, **CA 125:** glycoprotein 125, **CPT-11:** Irinotecan, **RF:** Riboflavin.

The type of cationic surfactant	Electrode type	Combined (nano) material	Analyte	Reference
CTAB	BDD electrode	–	BPA and HQ	[7]
	SPE	Zincon	PNL	[8]
	CPE	–	Alloxan	[15]
	GCE	CS	CA 125	[16]
	PGE	AuNPs	Cefixime	[17]
	PGE	MWCNT	CPT-11	[18]
SLS	PGCPE	CNT	RF	[20]
DTAB	CC electrode	–	Mb	[9]
DTAB and TTAB	CPE	MWCNT	dsDNA	[10]
DTAB	CPE	PPy-Fe_3O_4 nanoparticles	H_2O_2	[11]
DTAB and SDS	GCE	–	NRF	[12]
DTAB	CPE	PAn–SiO_2	H_2O_2	[13]
DTAB	Conductive paper	RGO and NFC	–	[14]
SDS	SPE	–	TFACl	[21]

of DTAB modified disposable electrochemical sensor and its application for environmental monitoring. It was aimed to fabricate a practical, robust, sensitive, selective, and inexpensive analytical tool for PNL monitoring due to the fact that it is an environmental hazard. First, the step-by-step modification of disposable PGEs by using a cationic surfactant, DTAB was performed, then the voltammetric monitoring of PNL was performed by using cyclic voltammetry (CV) technique in a short time as 45 s. Enhanced sensor response could be obtained by modification of PGEs using DTAB. The interference effects of organic and inorganic compounds on PNL detection were investigated, and the detection of PNL into tap water and industrial wastewater samples was studied. This is the first study in the literature in terms of DTAB modification of PGEs and PNL detection by using DTAB-PGEs.

2. Experimental

2.1. Apparatus

The voltammetric and impedimetric measurements were completed by using IVIUM Compactstate with IVIUM Release 4.951 software package (Holland). The electrochemical cell consisted of a working electrode as a pencil graphite electrode (PGE), a reference electrode as an Ag/AgCl/3 M KCl (BAS, Model RE-5B, W. Lafayette, USA), and a counter electrode as platinum wire. The used portion of a graphite lead (Tombow, Japan) was 14 mm and this part was holded by a pencil. 10 mm of the graphite lead was immersed into the surfactant sample or measurement solution. The pencil was holded with a metallic wire to obtain electrical contact [22,23].

2.1.1. Voltammetric measurements

Cyclic voltammetry (CV) technique was applied to monitor the step-by-step activation/modification processes of the PGEs based on the changes at the anodic peak current value (I_a) of $K_4[Fe(CN)_6$. For this purpose, 2.00 mM $K_3[Fe(CN)_6]/K_4[Fe(CN)_6]$ (1:1) contained in 0.10 M KCl was used as the anionic redox probe. The potential range was chosen between −0.45 V to +1.20 V with the scan rate as 50 mV s^{-1}.

2.1.2. Impedimetric measurements

2.00 mM $K_3[Fe(CN)_6]/K_4[Fe(CN)_6]$ (1:1) prepared in 0.10 M KCl was used for impedimetric measurements. The conditions for the impedimetric measurements were performed using the frequency ranging from 100 mHz to 100 kHz divided into 98 logarithmically equidistant points During the impedimetric measurement, +0.23 V as open circuit potential with a sinusoidal signal as 10 mV was applied. The charge-transfer resistance (R_{ct}) was measured using the Randles circuit. The elements of the circuit are R_{ct}, R_s, Q, and C which are representing the respective semicircle diameter, the solution resistance, the capacitance, and the Warburg impedance, respectively.

2.2. Chemicals

Dodecyltrimethylammonium bromide (DTAB), hexadecyltrimethylammonium bromide (CTAB), phenol (PNL), $CaCl_2$, $CuSO_4$, $MgSO_4$, $ZnSO_4$, $FeSO_4$, $HgCl_2$, potassiumhexacyanoferrate(III) ($K_3Fe(CN)_6$), potassiumhexacyanoferrate(II) trihydrate ($K_4Fe(CN)_6.3H_2O$), potassium chloride (KCl), dimethyl sulfoxide (DMSO), 2,4-dichlorophenoxyacetic acid (2,4-D), 2,6-di-tert-butyl-4-methylphenol (m-PNL), bisphenol A (BPA), D(+) glucose and urea were supplied from Sigma-Aldrich. Vitamin C (vitC), paracetamol (PRL), diclofenac sodium (DFC) were purchased from local drugstore.

Analytical grade chemicals were used for all study and they were supplied from Sigma–Aldrich. All solutions were prepared in ultra pure water.

2.3. Procedure

2.3.1. Preparation of the surfactant solutions

1000 μg/mL DTAB or CTAB was prepared in 50 mM phosphate buffer solution (buffer-1, pH 7.40) or ultrapure water for immobilization at the surface of electrochemically pretreated PGEs.

500–2000 μg/mL DTAB was prepared in DMSO to immobilize at the surface of unpretreated and chemically activated PGEs.

2.3.2. Preparation of PNL solution and the interference factors

1000 μg/mL of PNL, urea, D(+)glucose, vitC, PRL and DFC were prepared in buffer-1(pH 7.40) and 1000 μg/mL 2,4-D, m-PNL and BPA were prepared in DMSO as the stock solutions. 25–100 μg/mL and 1–5 μg/mL of PNL were prepared in buffer-1 (pH 7.40). 5 or 7.50 μg/mL interference factors were prepared in buffer-1 (pH 7.40).

For tap water and wastewater studies, PNL samples were spiked [24,25] into tap water or industrial wastewater samples from 1000 μg/mL stock solution of PNL prepared in buffer-1 (pH 7.40). The concentration level of PNL was 1–5 μg/mL. Tap water samples were obtained in the Bilecik Şeyh Edebali University region. The wastewater, used in the current study, was obtained from the landfill leachate pool of a solid waste management facility in Çanakkale province (40°10'29''N 26°32'37''E).

2.4. Surface modification of the sensor

2.4.1. Electrochemical pretreatment of PGEs (e-PGEs)

+1.40 V potential was applied for 30 s in 0.50 M acetate buffer containing 20 mM NaCl (buffer-2, pH 4.80) [26] to activate the electrodes and obtain a carboxylated surface.

2.4.2. Immobilization of CTAB or DTAB at the surface of e-PGEs

e-PGEs were dipped into 100 μL of 1000 μg/mL DTAB or CTAB prepared in buffer-1 (pH 7.40) for 15 min. Then, the electrodes were washed with buffer-1 (pH 7.40) during 5 s to eliminate unspecific binding of the surfactants.

2.4.3. Chemical activation of the PGEs

e-PGEs or unpretreated PGEs were dipped into 100 μL of 1 M NaOH

solution during 1 h for the formation of carboxyl groups at the graphite surface [27]. The PGEs were washed with ultrapure water at the end of the immobilization time.

2.4.4. Immobilization of DTAB at the surface of chemically activated PGEs

Chemically activated PGEs were dipped into 100 μL of DTAB solution prepared in DMSO for 1 h. Then, the electrodes were dried upward position for 5 min. The experiments were performed at room temperature and dark condition.

For stability test, DTAB-PGEs were stored for 5 days at room temperature and dark conditions.

2.5. Detection of PNL

Three-electrode system was immersed into 2 mL of the PNL sample, the oxidation signal of PNL was monitored at +0.660 V peak potential using CV technique. The potential range is from +0.30 V to +1.10 V with the scan rate as 50 mV s^{-1}.

3. Results and discussion

First, the modification of the PGEs using different cationic surfactants was investigated (Fig. S1). 1000 μg/mL DTAB (Fig. S1-B,b) or CTAB (Fig. S1-B,c) was modified at the e-PGE surface for 15 min and CV measurements were performed in the anionic redox probe. Although CTAB was widely used for modification of the carbon electrodes [8, 15–18], DTAB gave the highest anodic peak current (I_a) value by using the passive adsorption process (Fig. S1A,c) and the average I_a value was measured as 116.63 ± 4.27 μA with the relative standard deviation% (RSD%) as 3.66% (n = 3). Compared to the average I_a value obtained by e-PGEs (Fig. S1-B,a) there was a 14.45% increase at the average I_a value after DTAB modification of e-PGEs (Fig. S1-B,b). The effect of solvent for DTAB preparation was then investigated (Fig. S2). The highest average I_a value could be obtained using DTAB prepared in DMSO (Fig. S2-B,d). The increase at the average I_a values was calculated as 17.73% compared to the one obtained by e-PGEs (Fig. S2B-a). Therefore, DTAB was prepared in DMSO for further studies. Peyre et al. [24] studied the micellization characteristics of DTAB in water and water-DMSO solutions. According to the results of this study, the increasing DMSO concentration caused augmentation of the critical micelle concentration (CMC), decreased the aggregation number, and increased the ionization degree [28].

The modification of DTAB caused an increase at the I_a value due to its cationic structure [29]. Surfactants are surface-active molecules which means that they have ability to change electron transfer occurred between electrode/electrolyte interface [15,30]. Cationic surfactant modification caused to form an adsorptive layer at the graphite surface which had attractive behavior for electron transfer [15,31]. The increase at the I_a value after DTAB modification was consistent with the literature knowledge [10]. However, this increase was small even if DTAB concentration increased or the modification time was longer than 15 min. Therefore, chemical activation of PGEs was investigated (Fig. 1). The e-PGEs or unpretreated PGEs (the PGEs without electrochemical pretreatment) were chemically activated in the presence of 1 M NaOH and then 1000 μg/mL DTAB prepared in DMSO was immobilized at the surface of these electrodes during 1 h. After chemical activation of e-PGEs or unpretreated PGEs, the average I_a values decreased as 5.71% (Fig. 1C-I, a to c) and 21.96% (Fig. 1C-II, a to c), respectively as a result of the carboxylation of the surface of e-PGEs and unpretreated PGEs. However, carboxylation of the unpretreated PGEs was more effective

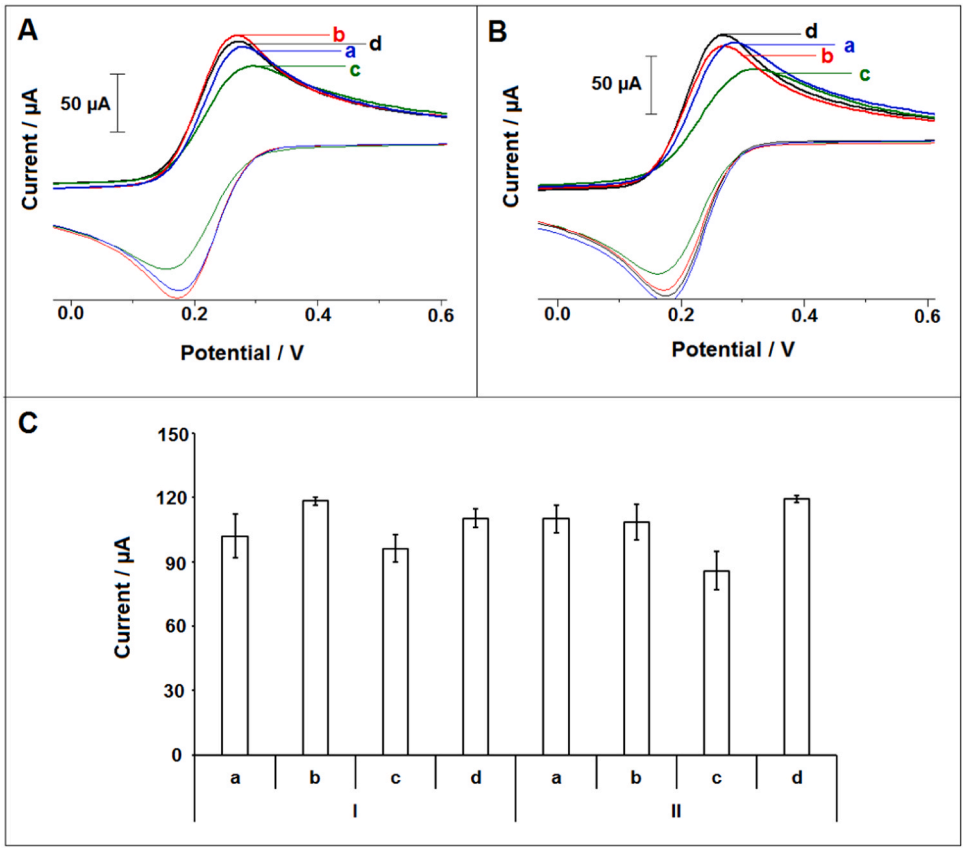

Fig. 1. The voltammograms and histograms representing the average I_a values of e-PGEs **(A, C-I)** or unpretreated PGEs **(B, C-II)**. e-PGE or unpretreated PGE **(a)**, 1000 μg/mL DTAB modified e-PGE or unpretreated PGE **(b)**, chemically activated e-PGE or unpretreated PGE **(c)**, 1000 μg/mL DTAB modified chemically activated e-PGE or unpretreated PGE **(d)**.

than e-PGEs. The average I_a value was found to be 85.78 ± 8.92 μA with the RSD% as 10.40% (n = 3) by using chemically activated unpretreated PGEs (Fig. 1C-II,c). 1000 μg/mL DTAB modification caused the increase at the average I_a value obtained by e-PGEs (Fig. 1C-I, a to b), chemically activated e-PGEs (Fig. 1B-I, c to d) or chemically activated unmodified PGEs (Fig. 1C-II, c to d). On the other hand, almost no change was observed at the average I_a value after the modification of DTAB onto unpretreated PGEs (Fig. 1C-II, a to b). The highest increase at the average I_a value could be obtained after the modification of chemically activated unpretreated PGEs. This increase may be attributed the successfull carboxylation of the PGE surface by using a chemical activation process and unpretreated PGEs, and DTAB molecules effectively bound onto the surface of carboxylated PGEs by the formation of covalent bindings between methyl groups of DTAB and carboxyl groups of the graphite surface. The increase ratio was calculated as 38.97% and the average I_a value was measured as 119.21 ± 1.54 μA (RSD% = 1.29%, n = 3) (Fig. 1 C-II, d). The peak-to-peak separation (ΔE_p) values of before and after the chemical activation of unpretreated PGE and DTAB modified PGE were found to be 100 mV, 160 mV, and 100 mV which means while chemical activation was the irreversible process andthe modification of DTAB had quasi-reversible behavior [32,33]. The average anodic charge values (Q_a) were found to be 6.78×10^{-4}, 6.24×10^{-4} and 6.7×10^{-4} C with the RSDs% as 4.33%, 7.54%, 2.79% (n = 3) by using unpretreated PGEs, chemically activated unpretreated PGEs and 1000 μg/mL DTAB modified PGEs, respectively. The changes at the Q_a values were in parallel with the changes at the average I_a values. Further experiments were performed with chemically activated unpretreated PGEs.

The chemical activation and DTAB modification of the PGEs were monitored by scanning electron microscopy (SEM) technique (Fig. 2). Layered graphite structure was seen at Fig. 2-A, and the changes occurred after chemical activation were determined in terms of the changes at the layered structure (Fig. 2, A-a to B-a). DTAB modification made smoother surface (Fig. 2-C) which indicated the successful modification of DTAB molecules at the surface of PGE.

The optimization of DTAB concentration was done using 500–2000 μg/mL DTAB and the average I_a values and related voltammograms were represented in Fig. 3. The highest I_a was obtained in the presence of 1500 μg/mL DTAB (Fig. 3-A,B,d) and the average I_a was measured as 123.96 ± 3.18 μA (RSD% = 2.56%, n = 3). 1500 μg/mL concentration level of DTAB was chosen as optimum.

The effective surface area (A_{eff}) values of the unpretreated PGE, chemically activated PGE and 1500 μg/mL DTAB modified PGE were calculated using Randles and Sevcik Equation [34] (Eq. 1):

$$i_p = 2.6910^5 n^{3/2} A_{eff} D^{1/2} C v^{1/2} \quad (1)$$

In this equation n, D and C represents the transferred electron number, the diffusion coefficient of $K_4[Fe(CN)_6]$ as 7.6×10^{-6} cm^2 s^{-1}, and the concentration of $K_4[Fe(CN)_6]$, respectively.

The A_{eff} values of unpretreated PGE, chemically activated PGE and 1500 μg/mL DTAB modified PGE were found to be 0.335, 0.259, 0.376 cm^2, respectively. The changes at the A_{eff} values were in a good agreement with the changes at the average I_a values. Also, the A_{eff} value was a good indicator to show the enhanced surface area obtained by

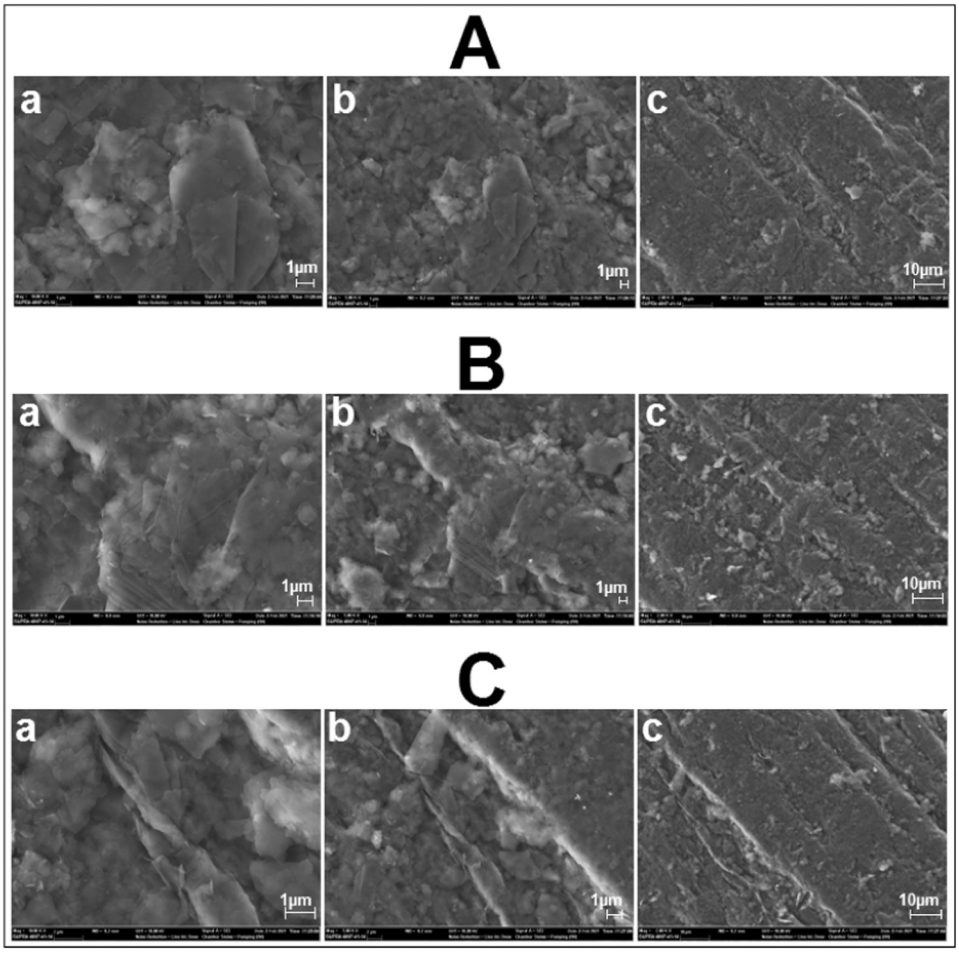

Fig. 2. SEM images of unpretreated PGE **(A)**, chemically activated PGE **(B)**, 1500 μg/mL DTAB modified PGE **(C)**. The acceleration voltage was 10.0 kV, the resolutions were 10000x **(a)**, 5000x **(b)** and 2000x **(c)**. All measurements were done at Bilecik Seyh Edebali University Research and Application Center.

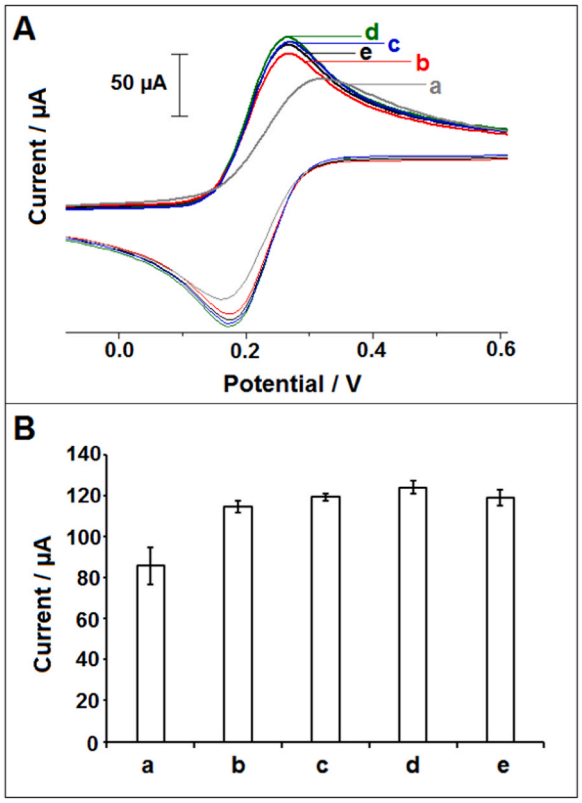

Fig. 3. The voltammograms **(A)** and histograms representing the average I_a values (n = 3) of chemically activated PGE **(a)**, 500 **(b)**, 1000 **(c)**, 1500 **(d)** and 2000 **(e)** µg/mL DTAB modified chemically activated PGE.

DTAB modification onto PGE.

The modification of DTAB at the PGE surface was also studied by electrochemical impedance spectroscopy (EIS) technique which made possible to evaluate the changes at the resistance against electron transfer occurred between electrode/electrolyte interface (Fig. S3) [35]. After modification of 1500 µg/mL DTAB onto the chemically activated PGE surface, the charge transfer resistance value (R_{ct}) sharply decreased (Fig. S3AB-a to b) as a result of the presence of DTAB molecules onto graphite surface. The electrode surface became positively charged due to the cationic structure of DTAB [29] and the repulsive interaction between the PGE surface and anionic redox probe decreased. The average R_{ct} value was measured as 15.50 ± 0.71 Ohm (RSD% = 4.56%, n = 3) by using DTAB-PGEs (Fig. S3B-b). The impedimetric results were consistent with the voltammetric results. Also, electrochemical results were in a good agreement with the microscopic results (Fig. 2).

In the second part of the study, PNL was monitored by using DTAB-PGEs. First, 25–100 µg/mL PNL was measured using chemically activated PGEs (Fig. S4) or DTAB-PGEs (Fig. S5). The PNL oxidation signal coming from +0.660 V increased till the concentration of PNL increased by using both chemically activated PGEs and DTAB-PGEs. In comparison to the PNL signals obtained by chemically activated PGEs, increased PNL signal could be measured at all concentration levels using DTAB-PGEs The average PNL signals obtained by both chemically activated PGEs and DTAB-PGEs and the increase ratios at the PNL signals were given in Table S1. The increase ratio increased when PNL concentration increased due to the fact that DTAB modification enhanced the electrode surface area for binding of PNL molecules. In addition, negatively charged PNL molecules [36] bound with positively charged DTAB molecules decorated onto PGEs. Calibration curves were obtained based on the average PNL signals obtained by chemically activated PGEs (Fig. S4B) or DTAB-PGEs (Fig. S5B). At 25–100 µg/mL concentration level, the detection limit (DL) values were estimated using 3 sb/m equation (sb represents the standard deviation of the blank and m is the slope of the equation of the analytical curve) [37] and found to be 10.45 and 8.31 µg/mL by using chemically activatedPGEs and DTAB-PGEs, respectively.

The detection of 1–5 µg/mL PNL was studied in order to show the capability of the proposed method to obtain a linear calibration curve even if in the presence of a low concentration of the analyte by using DTAB-PGEs (Fig. 4). The PNL oxidation signal was measured at +0.670 V in the presence of 1 µg/mL PNL and peak potential slightly shifted from positive to negative while PNL concentration increased. The electrochemical reaction depends on the mass transfer at the electrode/electrolyte interface. This transfer was easy at low concentrations of PNL, however, mass transfer was disrupted by adding more analyte in the measurement solution. Therefore, a slight shift at peak potential was observed. This result was consistent with the results reported by Arslan et al. [38]. The DL of PNL in buffer-1 (pH 7.40) was calculated at the concentration level ranging from 1 to 5 µg/mL and found to be 0.16 µg/mL (1.70 µM) [37] using the equation as y = 0.95x-0.44 with R^2 = 0.9988. This DL value was quite lower than the one reported as the maximum tolerated amount of PNL as 1 mg/L in drinking water [39]. The sensitivity was also calculated as 2.53 µA.mL/µg.cm^2.

3.1. Interference studies

Interference effects of both metal ions and organic compounds were investigated in the presence of the mixture of PNL:interference factor. Also, it was aimed to show how increase at the concentration of the interference factor affected on PNL signal. Therefore, the concentration levels were chosen as 5 µg/mL: 5 µg/mL or 5 µg/mL PNL: 7.50 µg/mL PNL:interference factor. Related results were given in Table 2 and Figs. S6 and S7. Since water sources could be contaminated by metal ions and PNL together [36], the interferences occurred in the presence of the metal ions were investigated. As seen in Table 2, the average PNL

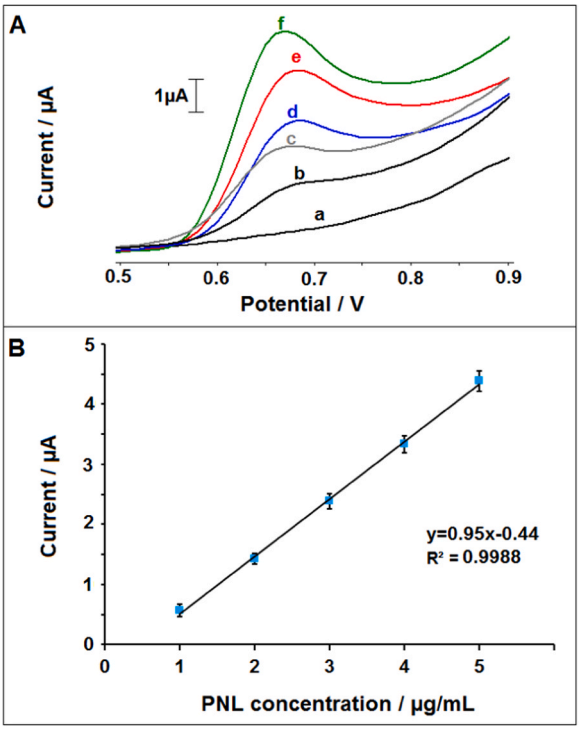

Fig. 4. The voltammograms **(A)** of DTAB-PGE **(a)**, PNL signals measured by DTAB-PGEs in the presence of 1 **(b)**, 2 **(c)**, 3 **(d)**, 4 **(e)** and 5 **(f)** µg/mL PNL in buffer-1 (pH = 7.40). Analytical curve **(B)** based on the PNL signals measured by DTAB-PGEs in the presence of 1–5 µg/mL PNL in buffer-1 (pH = 7.40) (n = 3).

Table 2
The average PNL signals measured at in the presence of 5 μg/mL PNL **(A)**, 5 μg/mL PNL:5 μg/mL interference factor **(B)** or 5 μg/mL PNL:7.50 μg/mL interference factor **(C)** (n = 3).

	A (μA)	B (μA)	C (μA)
PNL	4.62 ± 0.26		
PNL:Ca^{2+}		4.12 ± 0.22	5.23 ± 0.13
PNL:Cu^{2+}		4.20 ± 0.06	4.59 ± 0.77
PNL:Fe^{2+}		4.32 ± 0.01	5.48 ± 0.13
PNL:Hg^{2+}		4.41 ± 0.02	5.28 ± 0.25
PNL:Mg^{2+}		4.41 ± 0.10	5.38 ± 0.15
PNL:Zn^{2+}		4.32 ± 0.05	5.33 ± 0.24
PNL:2,4-D		4.52 ± 0.04	5.34 ± 0.06
PNL:m-PNL		4.29 ± 0.13	5.07 ± 0.18
PNL:urea		4.43 ± 0.15	5.25 ± 0.11
PNL:glucose		4.55 ± 0.02	5.23 ± 0.07
PNL:vitC		5.41 ± 0.27	5.18 ± 0.01
PNL:BPA		3.42 ± 0.15	2.64 ± 0.03
PNL:PRL		5.25 ± 0.12	5.56 ± 0.17
PNL:DFC		3.28 ± 0.37	2.30 ± 0.05

signal monitored at +0.660 V was measured as 4.62 ± 0.26 μA (RSD % = 5.26%, n = 3). There was no oxidation signal of the metal ions around +0.660 V peak potential (Fig. S6A to F, a). In the presence of 5 μg/mL metal ions, there was a small decrease at the PNL signal (Fig. S6A to F, c) and there was a small increase at the PNL signal in the presence of 7.50 μg/mL metal ions as well (Fig. S6A to F, d). There was an exception for Cu^{2+} ion, both concentration levels caused to monitor a small decrease at the PNL signal. Therefore, the interference effects of the metal ions on the PNL signal measured by DTAB-PGEs were negligible. Similar results were obtained in the presence of 2,4-D, m-PNL, urea, vitC, and glucose, none of them gave an oxidation signal around +0.660 V peak potential (Fig. S7A to E, a) and a little decrease at the PNL signal was observed in the presence of 5 μg/mL 2,4-D, m-PNL, urea, vitC, and glucose (Fig. S7A to E, c) while a small increase at the PNL signal was monitored in the presence of 7.50 μg/mL of them (Fig. S7A to E, d). The interference effects of bisphenol A (BPA), paracetamol (PRL), and diclofenac (DFC) were also investigated (Fig. S7F to H). There were oxidation signals of BPA, PRL and DFC at +0.500 V, +0.400 V and +0.550 V, respectively. The average oxidation signals of them were presented in Table 3. Two distinct oxidation peaks were observed in the presence of 5 μg/mL PNL: 5 μg/mL PRL or 5 μg/mL PNL: 7.50 μg/mL PRL (Fig. S7G), and there was a small increase at the PNL signal. Therefore, it could be evaluated that PRL did not significantly affect on PNL signal even if its concentration was the same with PNL or higher than PNL. Although the oxidation signals of BPA (Fig. S7F-a and b) or DFC (Fig. S7H-a and b) were close to the PNL signal due to their phenolic structure, PNL monitoring was achieved without fully coverage of the PNL signal by the BPA (Fig. S7G-f and g) or DFC signals (Fig. S7H-f and g). The PNL signal was observed even if the concentration of BPA or DFC increased. Therefore, it could be concluded that the developed electrochemical sensor had selective behavior against metal ions, organic compounds or phenolic compounds.

3.2. Stability and repeatability of DTAB-PGEs

In order to evaluate the stability of the developed electrochemical sensor, 5 μg/mL PNL was measured by freshly prepared (Fig. S8-a) or five days-stored (Fig. S8-b) DTAB-PGEs, and the average PNL signals were found to be 4.62 ± 0.26 μA (RSD% = 5.26%, n = 3) and 4.69 ± 0.63 μA (RSD% = 13.51%, n = 3), respectively. DTAB-PGEs were stable during 5 days as no signal loss was observed by using five days-stored DTAB-PGEs.

Repeatability of DTAB-PGEs was tested by preparing 5 different experimental groups which included three repetitive measurements. The average PNL signals were presented in Fig. S9 and measured as 4.54 ± 0.51 μA, 4.39 ± 0.19 μA, 4.75 ± 0.28 μA, 4.49 ± 0.19 μA, and 4.80 ± 0.29 μA with the RSD% values as 11.14%, 4.30%, 5.94%, 4.13%, 6.02%, respectively. These results showed that repeatable results could be obtained by using DTAB-PGEs.

Table 3
The average oxidation signals of BPA, PRL or DFC measured by DTAB-PGEs (n = 3). Measurements were done in the presence of 5 **(A)** or 7.50 μg/mL **(B)** BPA, PRL or DFC or 5 μg/mL: 5 μg/mL **(C)** or 5 μg/mL: 7.50 μg/mL PNL:BPA, PRL or DFC **(D)**.

	A	B	C	D
BPA	4.07 ± 0.15	5.96 ± 0.11	1.49 ± 0.31	2.32 ± 0.06
PRL	1.80 ± 0.18	1.99 ± 0.45	1.77 ± 0.10	2.66 ± 0.01
DFC	3.26 ± 0.45	6.08 ± 0.42	1.00 ± 0.28	2.57 ± 0.11

3.3. Real sample analysis

The voltammetric detection of PNL in tap water (Fig. 5) and industrial wastewater (Fig. 6) was investigated. In tap water, a linear increase at the PNL signal could be achieved using 1–5 μg/mL concentration range and the DL was found to be 0.12 μg/mL (1.26 μM) with the equation as y = 0.85x − 0.21 (R^2 = 0.9992) (Fig. 5B) [37] and the sensitivity was calculated as 2.26 μA.mL/μg.cm^2.

The detection of PNL into industrial wastewater was also investigated using a 1–5 μg/mL concentration range (Fig. 6). There was a background signal coming from wastewater (Fig. 6A-a) at +0.660 V and the average value of this signal was 0.40 ± 0.05 nA (RSD% = 12.76%, n = 3). The signal measured at +0.660 V increased till the concentration of PNL increased (Fig. 6A, b to e) which indicated this signal is the PNL signal and wastewater contained PNL. The analytical curve could be obtained at 0–4 μg/mL concentration level (Fig. 6B). The DL was calculated as 0.24 μg/mL (2.85 μM) using the equation as y = 0.34x + 0.44 (R^2 = 0.9975) [37]. The sensitivity was calculated as 0.90 μA.mL/μg.cm^2. It was reported that the concentration of PNL and its derivatives is able to range from 0.1 to 3900 mg/L in wastewater [40]. The DL value obtained in industrial wastewater was in the range of this reported concentration range.

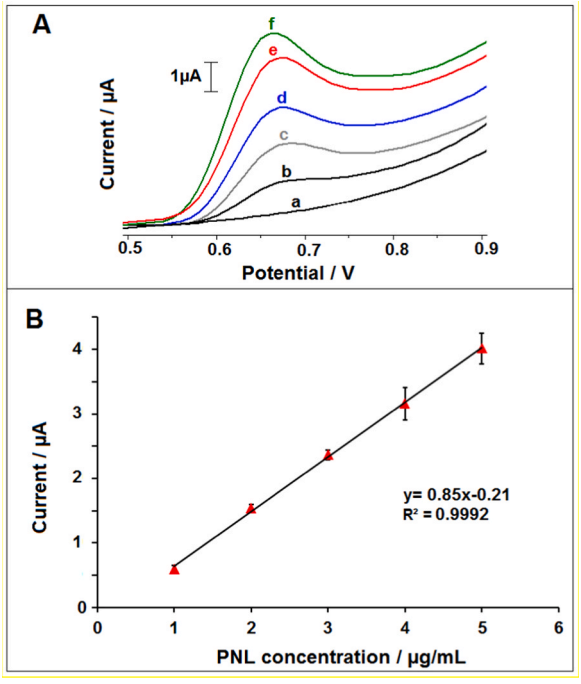

Fig. 5. The voltammograms **(A)** of tap water **(a)**, the PNL signals of 1 **(b)**, 2 **(c)**, 3 **(d)**, 4 **(e)** and 5 **(f)** μg/mL PNL prepared in tap water. Analytical curve **(B)** of the average PNL signals of 1–5 μg/mL PNL prepared in tap water (n = 3). All measurements were performed by DTAB-PGEs.

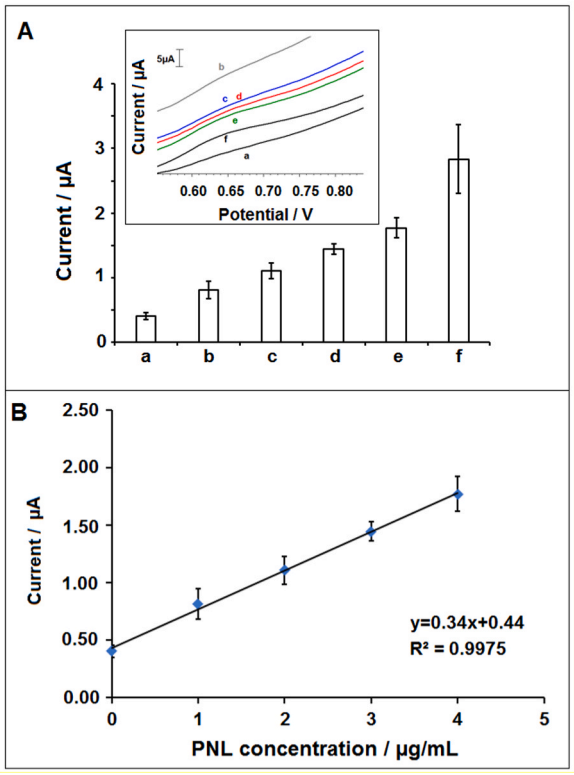

Fig. 6. The histograms **(A)** representing the average signal of industrial waste water **(a)**, the PNL signals by adding 1 **(b)**, 2 **(c)**, 3 **(d)**, 4 **(e)** and 5 **(f)** µg/mL PNL into the waste water. **Inset** was the voltammograms of industrial waste water **(a)**, 1 **(b)**, 2 **(c)**, 3 **(d)**, 4 **(e)** and 5 **(f)** µg/mL PNL**.** Analytical curve **(B)** based on the average PNL signals obtained in the presence of 0–4 µg/mL PNL prepared in industrial waste water . All measurements were done by DTAB-PGEs.

Some of the electrochemical sensor platforms developed for the detection of PNL were summarized in Table 4 [8,24,25,41–49]. DTAB modified PGEs allowed to detect PNL in not only buffer solution but also tap water and wastewater. Although some of the reports presented lower DLs than the one obtained in this study, the DLs were calculated in only buffer solution. However, low detection limits were achieved in different water samples by using DTAB-PGEs developed within the scope of this study. The application of DTAB-PGEs for PNL detection was successfully shown in real samples without any pretreatment of the samples such as ultrasonic water bath [42], pH adjustment [24], or filtering [25,45].

The authors want to underline how practical to develop PGE based electrochemical tools to monitor target (bio)molecules. GCE [25,42] and CPE [45] based electrochemical PNL sensors require labor-intensive and exhausting pretreatment steps of the electrodes such as grinding, filling, polishing, and sonication. In comparison to these electrodes, chemical activation of PGEs was done by a simple passive adsorption process, the electrodes were dipped into the sample for 1 h. The preparation of the DTAB-PGEs required to use of just 100 µL sample for each activation/modification step. Therefore, the disposable DTAB-PGEs could be fabricated with the minimum environmental burden. The use of PGEs was very practical, the experiments were performed by using pencil leads which could be purchased from local markets and the leads were introduced into the electrochemical cell by holding a pencil. Also, this is the first study in the literature about preparation of DTAB modified PGEs.

Economical features of the sensor systems should be discussed to evaluate the application of the analytical tools in the real world. PGEs make it possible to develop affordable sensor systems without the requirement of complicated preparation steps. Also, PGEs serve a large surface area for immobilization/adsorption of the (bio)molecules which leads to perform sensitive detection of the target.

In light of the explanations given above, it was proven that the successfull modification of PGE using DTAB and the potential analytical application of DTAB-PGE by performing voltammetric PNL detection was achieved.

4. Conclusion

This report represents a novel surfactant-based disposable sensor platform for electrochemical detection of PNL. The single-use electrochemical sensor could be fabricated by modification of DTAB onto PGEs using the passive adsorption process as the first time in the literature. Sensitive and selective electrochemical detection of PNL was successfully achieved. The application of the sensor platform was proven by performing the detection of PNL into tap water and industrial

Table 4
The electrochemical sensor platforms for detection of PNL. **Abbreviations: PEDOT:** poly(3,4-ethylenedioxythiophene), **poly HQVHMs:**poly (hydroquinone-oxovanadium (IV)) porous hollow microspheres (poly HQVHMs), **DAB:** 3,3′-diaminobenzidine, **NPG:** Nanoporous gold, **GTC:** Graphene modified anatase TiO2-carbon paste electrode, **µTED:** Thread-based electroanalytical device, **EASPCE:** Electrochemically activated screen printed electrode, **Ni/Al LDH/Pt:** Ni/Al Layered Double Hydroxide (LDH) thin film modified platinum electrode, **NiZn-MOF NSs:** 2D bimetallic metal organic framework nanosheets, **CA:** Chronoamperometry, **DPV:** Differential pulse voltammetry.

Electrode type	Detection method	Detection limit	Real sample analysis	Pretreatment of real samples	Ref.
CTAB-Zincon-SPE	CA	214 ppb in buffer	Waste water	–	[8]
SWCNT/PEDOT/ SPE	CV	0.38 µM in buffer	Distilled water and tap water	–	[41]
DAB-GCE	CV	1.0×10^{-10} M in buffer	Tap water	Ultrasonic water bath	[42]
GTC	CV	3.66×10^{-5} µM	–	–	[43]
CPE/poly HQVHMs	CV	30 nM in buffer	Tap water and river water	pH adjustment	[24]
µTED	CV	2.94 nmol/L in buffer	Tap water	–	[44]
Zincon-CPE	CV	9×10^{-6} mol/ L in buffer	Waste water	Filtration	[45]
NPG thin film	Amperometry	0.5 µM in buffer	–	–	[46]
EASPCE	DPV	–	Industrial pollutant absorbed molecular sieves	–	[47]
Ni/Al LDH/Pt	CA	–	–	–	[48]
NiZn-MOF NSs/ GCE	Amperometry	6.5 nM in buffer	Tap water	Filtration	[25]
PGE	DPV	120 nM in buffer	Insulin	–	[49]
DTAB-PGE	CV	0.16 µg/mL in buffer 0.12 µg/mL in tap water, 0.24 µg/mL in waste water	Tap water, waste water	–	This work

wastewater. DTAB modification of the single-use PGEs resulted in the sensitive detection than the one obtained by unmodified PGEs and the interference factors were eliminated by using DTAB-PGEs. The pros and cons of the sensor platform were comprehensively discussed by comparing with the previous electrochemical sensor platforms reported in the literature. DTAB-PGEs based electrochemical sensor platform is able to be a model for the development of miniaturized and microfluidic chip devices for detection of not only PNL but also different environmental and food contaminants.

CRediT authorship contribution statement

Gulsah Congur: Conceptualization, Methodology, Investigation, Implementation of all experimental procedures, Writing - original draft, Writing - review & editing, Visualization. **Ülküye Dudu Gül:** Conceptualization, Writing - original draft, Writing - review & editing, Resources.

Declaration of Competing Interest

There is no conflict of interest.

Acknowledgements

This study was partially supported by Bilecik Seyh Edebali University Scientific Research Project Coordination (Project number: 2020-01. BŞEÜ.12-02).

Appendix A. Supporting information

Supplementary data associated with this article can be found in the online version at doi:10.1016/j.jece.2021.105804.

References

[1] S.M. Shaban, J. Kang, D.H. Kim, Surfactants: recent advances and their applications, Compos. Commun. 22 (2020), 100537, https://doi.org/10.1016/j.coco.2020.100537.
[2] H.Y. Wu, C.L. Shih, T. Lee, T.Y. Chen, L.C. Lin, K.Y. Lin, H.C. Chang, I.C. Chuang, S. Y. Liou, P.C. Liao, Development and validation of an analytical procedure for quantitation of surfactants in dishwashing detergents using ultra-performance liquid chromatography-mass spectrometry, Talanta 194 (2019) 778–785, https://doi.org/10.1016/j.talanta.2018.10.084.
[3] M. Zhao, W. Lv, Y. Li, C. Dai, X. Wang, H. Zhou, C. Zou, M. Gao, Y. Zhang, Y. Wu, Study on the synergy between silica nanoparticles and surfactants for enhanced oil recovery during spontaneous imbibition, J. Mol. Liq. 261 (2018) 373–378, https://doi.org/10.1016/j.molliq.2018.04.034.
[4] D. Steinhilber, M. Witting, X. Zhang, M. Staegemann, F. Paulus, W. Friess, S. Küchler, R. Haag, Surfactant free preparation of biodegradable dendritic polyglycerol nanogels by inverse nanoprecipitation for encapsulation and release of pharmaceutical biomacromolecules, J. Control. Release 169 (3) (2013) 289–295, https://doi.org/10.1016/j.jconrel.2012.12.008.
[5] M. Hasheminejad, A. Nezamzadeh-Ejhieh, A novel citrate selective electrode based on surfactant modified nano-clinoptilolite, Food Chem. 172 (2015) 794–801, https://doi.org/10.1016/j.foodchem.2014.09.057.
[6] N. Asikin-Mijan, Y.H. Taufiq-Yap, H.V. Lee, Synthesis of clamshell derived $Ca(OH)_2$ nano-particles via simple surfactant-hydration treatment, Chem. Eng. J. 262 (2015) 1043–1051, https://doi.org/10.1016/j.cej.2014.10.069.
[7] S.A. Hoshyar, H.A.H. Barzani, Y. Yardım, Z. Sentürk, The effect of CTAB, a cationic surfactant, on the adsorption ability of the boron-doped diamond electrode: application for voltammetric sensing of bisphenol A and hydroquinone in water samples, Colloids Surf. A Physicochem. Eng. Asp. 610 (2021), 125916, https://doi.org/10.1016/j.colsurfa.2020.125916.
[8] M. Hosseini Aliabadi, N. Esmaeili, H.S. Jahromi, An electrochemical composite sensor for phenol detection in waste water, Appl. Nanosci. 10 (2020) 597–609, https://doi.org/10.1007/s13204-019-01139-6.
[9] Y.Z. Zhou, H. Wang, S.Y. Dong, A.X. Tian, Z.X. He, B. Chen, Direct electrochemistry and electrocatalysis of myoglobin in dodecyltrimethylammonium bromide film modified carbon ceramic electrode, Chin. Chem. Lett. 22 (2011) 465–468, https://doi.org/10.1016/j.cclet.2010.11.012.
[10] C. Serpi, A. Voulgaropoulos, S. Girousi, Electroanalysis use of cationic surfactants film carbon paste electrodes modified with multiwalled carbon nanotubes in electrochemical analysis of dsDNA, Electroanalysis (2013) 2493–2499, https://doi.org/10.1002/elan.201300339.
[11] Y. Zhou, H. Zhang, J. Zhang, J. Zheng, Direct electrochemistry and electrocatalysis of hemoglobin on polypyrrole-Fe_3O_4/dodecyltrimethylammonium bromide-modified carbon paste electrode and its biosensing for hydrogen peroxide, Biocatal. Biotransform. 31 (2013) 313–322, https://doi.org/10.3109/10242422.2013.858709.
[12] M. Sohail, H.M. Abd Ur Rahman, M.N. Asghar, S. Shaukat, Volumetric, acoustic, electrochemical and spectroscopic investigation of norfloxacin–ionic surfactant interactions, J. Mol. Liq. 318 (2020), 114179, https://doi.org/10.1016/j.molliq.2020.114179.
[13] B. Chen, H. Wang, H. Zhang, Z. He, S. Zhang, T. Liu, Y. Zhou, A novel hydrogen peroxide sensor based on hemoglobin immobilized PAn–SiO_2/DTAB composite film, J. Mol. Liq. 171 (2012) 23–28, https://doi.org/10.1016/j.molliq.2012.04.007.
[14] T. Ardyani, A. Mohamed, S.A. Bakar, M. Sagisaka, Y. Umetsu, M.H. Mamat, M. Khairul Ahmad, H.P.S.A. Khalil, S.M. King, S.E. Rogers, J. Eastoe, Electrochemical exfoliation of graphite in nanofibrillated kenaf cellulose (NFC)/surfactant mixture for the development of conductive paper, Carbohydr. Polym. 228 (2020), 115376, https://doi.org/10.1016/j.carbpol.2019.115376.
[15] A.B. Monnappa, J.G. Manjunatha, A.S. Bhatt, Design of a sensitive and selective voltammetric sensor based on a cationic surfactant-modified carbon paste electrode for the determination of alloxan, ACS Omega 36 (2020) 23481–23490, https://doi.org/10.1021/acsomega.0c03517.
[16] M. Hasanzadeh, A. Mohammadzadeh, M. Jafari, B. Habibi, Ultrasensitive immunoassay of glycoprotein 125 (CA 125) in untreated human plasma samples using poly (CTAB-chitosan) doped with silver nanoparticles, Int. J. Biol. Macromol. 120 (2018) 2048–2064, https://doi.org/10.1016/j.ijbiomac.2018.09.208.
[17] P. Manjunatha, Y. Arthoba Nayaka, Cetyltrimethylammonium bromide-gold nanoparticles composite modified pencil graphite electrode for the electrochemical investigation of cefixime present in pharmaceutical formulations and biology, Chem. Data Collect. 21 (2019), 100217, https://doi.org/10.1016/j.cdc.2019.100217.
[18] G. Bolat, Investigation of poly(CTAB-MWCNTs) composite based electrochemical DNA biosensor and interaction study with anticancer drug irinotecan, Microchem. J. 159 (2020), 105426, https://doi.org/10.1016/j.microc.2020.105426.
[19] A. Nathani, N. Vishnu, C.S. Sharma, Review—pencil graphite electrodes as platform for enzyme and enzyme-like protein immobilization for electrochemical detection, J. Electrochem. Soc. 167 (2020), 037520, https://doi.org/10.1149/2.0202003JES.
[20] G. Tigari, J.G. Manjunatha, A surfactant enhanced novel pencil graphite and carbon nanotube composite paste material as an effective electrochemical sensor for determination of riboflavin, J. Sci. Adv. Mater. Devices 5 (2020) 56–64, https://doi.org/10.1016/j.jsamd.2019.11.001.
[21] T.A. Ali, M.H. Soliman, G.G. Mohamed, Electrochemical determination of N-(1,1,2,2- tetrahydroperfluorooctyl)-N,N-dimethylammonium chloride surfactant in different water samples using modified screen- printed electrode, Int. J. Electrochem. Sci. 11 (2016) 1055–1069.
[22] A. Erdem, B. Kosmider, R. Osiecka, E. Zyner, J. Ochocki, M. Ozsoz, Electrochemical genosensing of the interaction between the potential chemotherapeutic agent, cis-bis(3-aminoflavone)dichloroplatinum(II) and DNA in comparison with cis-DDP, J. Pharm. Biomed. Anal. 38 (2005) 645–652, https://doi.org/10.1016/j.jpba.2005.02.010.
[23] A. Erdem, P. Papakonstantinou, H. Murphy, Direct DNA hybridization at disposable graphite electrodes modified with carbon nanotubes, Anal. Chem. 78 (2006) 6656–6659, https://doi.org/10.1021/ac060202z.
[24] M. Shahbakhsh, H. Saravani, S. Narouie, Z. Hashemzaei, Poly (hydroquinone-oxovanadium (IV)) porous hollow microspheres for voltammetric detection of phenol, Microchem. J. 164 (2021), 105948, https://doi.org/10.1016/j.microc.2021.105948.
[25] Y. Wen, R. Li, J. Liu, X. Zhang, P. Wang, X. Zhang, B. Zhou, H. Li, J. Wang, Z. Li, B. Sun, Promotion effect of Zn on 2D bimetallic NiZn metal organic framework nanosheets for tyrosinase immobilization and ultrasensitive detection of phenol, Anal. Chim. Acta 1127 (2020) 131–139, https://doi.org/10.1016/j.aca.2020.06.062.
[26] A. Erdem, M. Muti, P. Papakonstantinou, E. Canavar, H. Karadeniz, G. Congur, S. Sharma, Graphene oxide integrated sensor for electrochemical monitoring of mitomycin C–DNA interaction, Analyst 137 (2012) 2129–2135, https://doi.org/10.1039/C2AN16011K.
[27] S. Guo, J. Raya, D. Ji, Y. Nishina, C. Ménard-Moyon, A. Bianco, Is carboxylation an efficient method for graphene oxide functionalization? Nanoscale Adv. 2 (2020) 4085–4092, https://doi.org/10.1039/D0NA00561D.
[28] V. Peyre, S. Bouguerra, F. Testard, Enhanced photocatalytic degradation of phenol and photogenerated charges transfer property over BiOI-loaded ZnO composites, J. Colloid Interface Sci. 389 (2013) 164–174, https://doi.org/10.1016/j.jcis.2017.01.064.
[29] V. Sharma, P. Cantero-López, O. Yañez-Osses, A. Kumar, Effect of cosolvents DMSO and glycerol on the self-assembly behavior of SDBS and CPC: an experimental and theoretical approach, J. Chem. Eng. Data 63 (2018) 3083–3096, https://doi.org/10.1021/acs.jced.8b00326.
[30] X. Dang, Y. Wei, S. Hu, Effects of surfactants on the electroreduction of dioxygen at an acetylene black electrode, Anal. Sci. 20 (2004) 307–310, https://doi.org/10.2116/analsci.20.307.
[31] B.M. Amrutha, J.G. Manjunatha, A.S. Bhatt, N. Hareesha, Electrochemical analysis of evans blue by surfactant modified carbon nanotube paste electrode, J. Mater. Environ. Sci. 10 (2019) 668–676.
[32] E.P. Randviir, A cross examination of electron transfer rate constants for carbon screen-printed electrodes using electrochemical impedance spectroscopy and cyclic

voltammetry, Electrochim. Acta 286 (2018) 179–186, https://doi.org/10.1016/j.electacta.2018.08.021.
[33] P. Qian, S. Ai, H. Yin, J. Li, Evaluation of DNA damage and antioxidant capacity of sericin by a DNA electrochemical biosensor based on dendrimer-encapsulated Au-Pd/chitosan composite, Microchim. Acta 168 (2010) 347–354, https://doi.org/10.1007/s00604-009-0280-x.
[34] T.E. Cummings, P.J. Elving, Determination of the electrochemically effective electrode area, Anal. Chem. 50 (1978) 480–488, https://doi.org/10.1021/ac50025a031.
[35] F. Ciucci, Modeling electrochemical impedance spectroscopy, Curr. Opin. Electrochem. 13 (2019) 132–139, https://doi.org/10.1016/j.coelec.2018.12.003.
[36] R. Zhao, Y. Li, J. Ji, Q. Wang, G. Li, T. Wu, B. Zhang, Efficient removal of phenol and p-nitrophenol using nitrogen-doped reduced graphene oxide, Colloids Surf. A Physicochem. Eng. Asp. 611 (2021), 125866, https://doi.org/10.1016/j.colsurfa.2020.125866.
[37] J.N. Miller, J.C. Miller. Statistics and Chemometrics for Analytical Chemistry, sixth ed., Pearson Education, Essex, 2005, pp. 121–123.
[38] G. Arslan, B. Yazici, M. Erbil, The effect of pH, temperature and concentration on electrooxidation of phenol, J. Hazard. Mater. 124 (2005) 37–43, https://doi.org/10.1016/j.jhazmat.2003.09.015.
[39] Rachna Rani M., U. Shanker, Sunlight assisted degradation of toxic phenols by zinc oxide doped prussian blue nanocomposite, J. Environ. Chem. Eng. 8 (2020), 104040, https://doi.org/10.1016/j.jece.2020.104040.
[40] O.G. Sas, P.B. Sánchez, B. González, Á. Domínguez, Removal of phenolic pollutants from wastewater streams using ionic liquids, Sep. Purif. Technol. 236 (2020), 116310, https://doi.org/10.1016/j.seppur.2019.116310.
[41] N. Negash, H. Alemu, M. Tessema, Flow injection amperometric determination of phenol and chlorophenols at single wall carbon nanotube modified glassy carbon electrode, Am. J. Anal. Chem. 5 (2014) 188–198, https://doi.org/10.4236/ajac.2014.53023.
[42] I.E. Mülazımoğlu, A. Demir Mülazımoğlu, E. Yılmaz, Determination of quantitative phenol in tap water samples as electrochemical using 3,3′-diaminobenzidine modified glassy carbon sensor electrode, Desalination 268 (2011) 227–232, https://doi.org/10.1016/j.desal.2010.10.033.
[43] M. Nurdin, L. Agusu, A.A.M. Putra, M. Maulidiyah, Z. Arham, D. Wibowo, M. Z. Muzakkar, A.A. Umar, Synthesis and electrochemical performance of graphene-TiO_2-carbon paste nanocomposites electrode in phenol detection, J. Phys. Chem. Solid 131 (2019) 104–110, https://doi.org/10.1016/j.jpcs.2019.03.014.
[44] F.R. Caetano, E.A. Carneiro, D. Agustini, L.C.S. Figueiredo-Filho, C.E. Banks, M. F. Bergamini, L.H. Marcolino-Junior, Combination of electrochemical biosensor and textile threads: a microfluidic device for phenol determination in tap water, Biosens. Bioelectron. 99 (2018) 382–388, https://doi.org/10.1016/j.bios.2017.07.070.
[45] W. Qin, X. Liu, H. Chen, J. Yang, Amperometric sensors for detection of phenol in oilfield wastewater using electrochemical polymerization of zincon film, Anal. Methods 6 (2014) 5734–5740, https://doi.org/10.1039/c3ay41855c.
[46] B.T.P. Quynh, J.Y. Byun, S.H. Kim, Non-enzymatic amperometric detection of phenol and catechol using nanoporous gold, Sens. Actuators B 221 (2015) 191–200, https://doi.org/10.1016/j.snb.2015.06.067.
[47] S. Sakthinathan, S. Palanisamy, S.M. Chen, P.S. Wu, L. Yao, B.S. Lou, Electrochemical detection of phenol in industrial pollutant absorbed molecular sieves by electrochemically activated screen printed carbon electrode, Int. J. Electrochem. Sci. 10 (2015) 3319–3328.
[48] E. Scavetta, A. Casagrande, I. Gualandi, D. Tonelli, Analytical performances of Ni LDH films electrochemically deposited on Pt surfaces: phenol and glucose detection, J. Electroanal. Chem. 722–723 (2014) 15–22, https://doi.org/10.1016/j.jelechem.2014.03.018.
[49] N. Vishnu, A.S. Kumar, A preanodized 6B-pencil graphite as an efficient electrochemical sensor for mono-phenolic preservatives (phenol and meta-cresol) in insulin formulations, Anal. Methods 7 (2015) 1943–1950, https://doi.org/10.1039/C4AY02798A.